

NASA Technical Paper 1522

NASA  
TP  
1522  
c.1

LOAN COPY RETURN TO  
AFWL TECHNICAL LIBRARY  
KIRTLAND AFB, N. M.

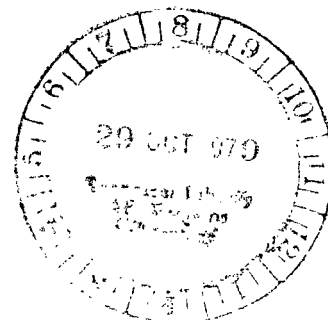
TECH LIBRARY KAFB, NM  
0134821

# Load Concentration Due to Missing Members in Planar Faces of a Large Space Truss

Joseph E. Walz

OCTOBER 1979

**NASA**





NASA Technical Paper 1522

# Load Concentration Due to Missing Members in Planar Faces of a Large Space Truss

Joseph E. Walz  
*Langley Research Center  
Hampton, Virginia*



National Aeronautics  
and Space Administration

**Scientific and Technical  
Information Branch**

1979

## SUMMARY

A large space structure with members missing was investigated using a finite-element analysis. The particular structural configuration was the tetrahedral truss, with attention restricted to one of its planar faces. Initially the finite-element model of a complete face was verified by comparing it with known results for some basic loadings. Then an analysis was made of the structure with members near the center removed. Some calculations were made on the influence of the mesh size of a structure containing a hexagonal hole, and an analysis was also made of a structure with a rigid hexagonal insert. In general, load-concentration effects in these trusses were significantly lower than classical stress-concentration effects in an infinitely wide isotropic plate with a circular hole or circular rigid inclusion, although larger effects were obtained when a hole extended over several rings of elements.

## INTRODUCTION

Large, low-mass structures are expected to play an important role in future space missions. These missions include activities such as solar power collection, navigation, Earth resource surveillance, and communications. A discussion of potential space activities is presented in reference 1, and a survey of expected requirements of large space structures is presented in reference 2. Although specific missions are not yet defined, some form of large, open truss structure is expected to be a strong candidate for providing a stiff skeletal frame upon which functions can be conducted in orbit. One such structure is a tetrahedral truss, or octetruss, sketched in figure 1. The tetrahedral truss, constructed of identical column members, has pseudo-isotropic elastic properties. Some design considerations for large space structures, such as the tetrahedral truss, are reported in references 3 and 4.

The present report examines the ability of this type of truss to function safely if one or more of the column members are damaged and unable to carry a load, a potential design problem not considered in reference 3 or 4. Such damage could result, for instance, from impact by meteoroids or space debris, assembly accidents, or docking accidents. In addition, effects that exceedingly stiff equipment might have when attached to the truss are investigated. A finite-element model of a tetrahedral truss with members missing from its isogrid planar faces or with a rigid insert simulating the stiff equipment was subjected to in-plane loadings. Load concentration induced as a consequence of the missing members or the rigid insert was investigated only in a two-dimensional framework. Since redundancy is added by the core members for the three-dimensional truss, the two-dimensional results tend to overestimate loads and are conservative for design of the three-dimensional truss.

The analytical tool used to obtain the results was the NASTRAN<sup>1</sup> computer program (ref. 5). Initially, attention was focused on a reference model of the two-dimensional structure with no missing members. To verify the model, comparisons were made with closed-form solutions of reference 3 for basic loading conditions of extension in each of two directions and shear. A representative portion of a large mesh with selected members removed was subsequently analyzed under the same extensional and shear loadings to obtain load-concentration factors. Load-concentration factors exhibited by a structure with missing members that formed a hexagonal hole are compared with classical stress-concentration factors in an infinitely wide isotropic plate with a circular hole. The effect of increasing the number of elements in the mesh with a constant-size hexagonal hole was determined. Load-concentration factors exhibited by a structure with a rigid hexagonal insert were also computed and are compared with stress-concentration factors in an isotropic plate with a rigid circular inclusion. Finally, the effect of increasing the number of members removed from the truss was examined.

#### SYMBOLS

$l$	length of member (see fig. 2)
$n$	number of members along an edge (see fig. 2)
$N_x, N_y$	direct loading per unit length in x- and y-directions (see fig. 3)
$N_{xy}$	shear loading per unit length (see fig. 3)
$P_{0^\circ}, P_{60^\circ}, P_{-60^\circ}$	loads in members inclined $0^\circ$ , $60^\circ$ , and $-60^\circ$ with respect to x-direction
$r_h$	"radius" of hexagonal hole or radius of circle that circumscribes hexagon
$x, y$	coordinate directions defined in figure 2

#### REFERENCE STRUCTURAL MODEL AND LOADINGS

##### Structural Model

As indicated previously, this study considers a planar face of a tetrahedral truss. The model of a planar face is an  $n \times n$  mesh shown in figure 2, where  $n$  is always an even number. The model is a two-dimensional assemblage of identical members (rod elements in the finite-element computer program) with pin joints assumed at the nodes. Constraints were chosen to restrain rigid-body motion without inducing additional loads into the members. For the full model, motion in both x- and y-directions was restrained at the node halfway between

---

<sup>1</sup>NASTRAN: Registered trademark of the National Aeronautics and Space Administration.

the top and bottom of the left edge, and motion in the y-direction only was restrained at the corresponding node on the right edge. Therefore, rigid-body rotation was restrained. Equivalent boundary conditions, except for uniform translation in the x-direction, were imposed on quarter-symmetry models of the structure.

### Loadings and Load Distributions for Reference Model

Internal member loads due to anticipated loadings in space are very low. Thermal loading and inertial loadings are likely to be determining factors for internal loads, but depend a great deal on equipment which is mounted to the truss. To aid in the understanding of the behavior of these large space structures without unduly complicating the present study, some basic loading conditions were considered.

The loading conditions, depicted in figure 3, are an essentially uniform loading in the x-direction  $N_x$ , a shear loading  $N_{xy}$ , a loading in the y-direction  $N_y$ , and a loading in the y-direction with some side loadings,  $N_y$  corrected. The loading  $N_x$  is not quite uniform since loads of equal magnitude were applied at all joints along the jagged edges, even at the top and bottom joints. The uniform loading with side loadings (fig. 3(d)) simulates the combined loading on a portion of a mesh infinite in both directions. This loading is referred to as  $N_y$  corrected. Discussion of this loading condition is presented subsequently.

Loading in x-direction.- For the reference model, individual member loads for the loading  $N_x$ , as taken from reference 3 and reproduced by the present infinite-element analysis, are

$$\frac{P_{0^{\circ}}}{N_x \ell} = \frac{\sqrt{3}}{2} \quad (1)$$

$$\frac{P_{60^{\circ}}}{N_x \ell} = 0 \quad (2)$$

$$\frac{P_{-60^{\circ}}}{N_x \ell} = 0 \quad (3)$$

where  $P_{0^{\circ}}$ ,  $P_{60^{\circ}}$ , and  $P_{-60^{\circ}}$  are the loads in members parallel, inclined  $60^{\circ}$ , and inclined  $-60^{\circ}$  to the x-direction, respectively. The x-direction is shown in figure 2. The chosen loading was applied by means of the system of concentrated loads shown in figure 3(a). Each of these loads had a magnitude of  $(\sqrt{3}/2)N_x \ell$ , including those at the top and bottom joints.

Shear loading.- For the uniform loading  $N_{xy}$ , the individual member loads, as taken from reference 3 and reproduced numerically by this study, are

$$\frac{P_{0^\circ}}{N_{xy}l} = 0 \quad (4)$$

$$\frac{P_{60^\circ}}{N_{xy}l} = 1 \quad (5)$$

$$\frac{P_{-60^\circ}}{N_{xy}l} = -1 \quad (6)$$

The uniform loading was applied by means of the concentrated loads shown in figure 3(b). Here loads of magnitude  $N_{xy}l$  were applied to joints on the top and bottom rows and loads of magnitude  $\sqrt{3} N_{xy}l$  were applied to the protruding joints on the jagged sides. At all corner joints, loads of half the magnitude of loads on the corresponding sides were applied.

Loading in y-direction.- For the uniform loading  $N_y$  on a doubly infinite mesh the individual member loads from reference 3 are

$$\frac{P_{0^\circ}}{N_y l} = -\frac{\sqrt{3}}{6} \quad (7)$$

$$\frac{P_{60^\circ}}{N_y l} = \frac{\sqrt{3}}{3} \quad (8)$$

$$\frac{P_{-60^\circ}}{N_y l} = \frac{\sqrt{3}}{3} \quad (9)$$

To reproduce these results numerically, special attention must be paid to the jagged edges. In figure 3(c), no loads on the jagged edges were considered, and in figure 3(d), side loads were considered. In both cases, loads of magnitude  $N_y l$  were applied at the joints on the top and bottom rows except at the corners where the magnitude was  $(1/2)N_y l$ .

Results for a quarter panel of the configuration of figure 3(c), which did not include any loads on the jagged edges, are shown in figure 4 for a  $16 \times 16$  full mesh. The results show edge effects; that is, member loads are significantly different from those of equations (7), (8), and (9) near the jagged edges, but tend toward these values near the center. The maximum member load is 27 percent larger than that predicted by equation (8). This edge effect occurs even when more members are added to the mesh. Note that in figure 4, as in all figures in this paper that display nondimensional member loads,  $Nl$  was chosen to be 1000 for convenience. The plot was produced by making a modification to the computer program described in reference 6.

For the loading,  $N_y$  corrected, edge loadings of magnitude  $(\sqrt{3}/6)N_y l$ , which represent the contribution of those members that would exist in a doubly infinite mesh, were applied at the joints along the jagged edges, as indicated in figure 3(d). Member loads for the configuration of figure 3(d) agree with those of equations (7), (8), and (9).

## RESULTS AND DISCUSSION

The member loads obtained in this study were nondimensionalized so that they are independent of Young's modulus, cross-sectional area, and length of the members, providing that the assumption of pinned joints remains valid. Models with members removed from the structure were analyzed. Two types of single members were removed: (1) a horizontal member near the center and (2) a diagonal member near the center. These two situations cover all possibilities of a single member being removed at the center of the truss. A model having an entire six-member unit about a central joint removed and a model having a center joint made rigid with the six-member unit made inextensible were also studied. Finally, additional results on models with more extensive hexagonal holes were obtained.

### Models With One Member Missing

The effects of removing a horizontal member in a  $16 \times 16$  mesh for the loadings,  $N_x$ ,  $N_y$ , and  $N_y$  corrected are shown in figures 5(a), 5(b), and 5(c), respectively. No results are shown for a shear loading because there were no changes in member loads from those predicted by equations (4), (5), and (6). As can be seen from figure 5(a), the member loads are almost symmetric about the center of the removed member. Notice that the effect of the removed member dissipates pretty rapidly, as indicated by the small values of load on the diagonals more than three member lengths from the removed member. A comparison of the two types of loading in the y-direction (figs. 5(b) and 5(c)) reveals essentially the same distribution of load except within three member lengths of the sides where the previously mentioned edge effects occur (compare figs. 4 and 5(b)).

Next, the  $16 \times 16$  mesh with a diagonal member removed was subjected to the four basic loading conditions. Member loads for the loadings  $N_{xy}$  and  $N_y$  are

shown in figures 6(a) and 6(b), respectively. No results are shown for the loading  $N_x$  because there are no changes in member loads from those predicted by equations (1), (2), and (3). No results are presented for the  $N_y$  corrected because of the similarity (except for edge effects) to those displayed in figure 6(b).

Maximum nondimensional member loads in the vicinity of the removed member (either horizontal or diagonal) are listed in table I. Presented also in this table is the load-concentration factor which is defined here to be the ratio of the maximum load in a member near the damaged area to the load in that same member for the undamaged condition. With a horizontal member removed, maximum member loads are 26 percent and 17 percent higher than loads in the reference model for extensional loadings in x- and y-directions, respectively. With a diagonal member removed, maximum member loads are 35 percent and 26 percent higher than loads in the reference model for shear loading and loading in the y-direction, respectively.

#### Models With Six Members Missing

An entire six-member unit about the center node of a  $16 \times 16$  mesh was removed to form a hexagonal hole, and the remaining structure was analyzed. The resulting maximum nondimensional member loads in the structure are presented in table I. The maximum loads increased by 30 percent and 47 percent for extensional loadings in the x- and y-directions, respectively, and by 56 percent for the shear loading. The graphic displays of all nondimensional member loads for three of the loading conditions are presented in figure 7. Because of the symmetry of the structure and either symmetry or antisymmetry of the loadings, only the upper right quadrant of the structure is shown.

Since the unbroken mesh exhibits isotropic behavior (see ref. 3 or 7), it is interesting to compare the present results with solutions of an infinitely wide isotropic plate with a circular hole at its center. As indicated in table I for extensional loadings, the classical plate stress-concentration factors would be 3.0 for extension in the x- and y-directions, and 4.0 for shear (see ref. 8). Thus the present load-concentration factors for the mesh are significantly lower than might be presumed. However, the two situations are not quite comparable since the location of maximum load for the mesh does not always correspond to the location of maximum stress concentration in the isotropic plate. For example, in the case of the shear loading, the maximum load in the mesh is in a diagonal member that joins a node on the boundary of the hole (fig. 7(b)), whereas classical stress concentration for shear loading is located on the edge of the hole.

A procedure for designing isogrid structures (the form of mesh considered here) with a cover plate with a hexagonal hole has been given in reference 7. If this procedure is attempted when no cover plate exists for large space structures, the results would be overly conservative since the procedure is based on classical stress-concentration effects for extension of an isotropic plate.

Additional studies were made on the model with a six-member unit removed to see whether any significant changes would occur as the size of the structure

increased. In these studies, the length of the members, and hence the size of the hole, were constant with the overall dimensions of the structure growing as the number of elements in the mesh along an edge was increased. Table II presents the results for various mesh sizes which indicate a slight decrease in maximum nondimensional loads and thus a slight decrease in load-concentration factors as the number of members in the mesh was increased. Plots of these data as a function of the reciprocal of the square of the mesh number are presented in figure 8 and are extrapolated to give some idea of convergence.

### Model With Rigid Insert

A  $16 \times 16$  mesh structure with a rigid insert was examined. The rigid insert was formed by rigidly connecting the center node to the adjacent six nodes and permitting no relative rotation between members at the center joint. Such a situation might simulate a piece of equipment being connected to the center and six adjacent joints. The solution was obtained with the MPC (multi-point constraint) feature in the finite-element analysis. The graphic displays of nondimensional member loads are presented in figure 9. Again only one quadrant of the structure is shown. Except for loading  $N_x$ , load-concentration factors are somewhat less than those which exist in the structure with the six-member unit removed. The classical stress-concentration factors for an infinitely wide isotropic plate with a rigid inclusion, as listed in table I, are obtained from reference 9 with Poisson's ratio taken to be  $1/3$  to be consistent with the present studies. For extensional and shearing loadings, this classical stress-concentration factor is 1.50, and load-concentration factors for the mesh range from 1.28 to 1.37. Thus, classical stress-concentration factors overestimate load-concentration factors for the mesh with the rigid insert, but not nearly as much as for the mesh with the hole.

### Models With Hexagonal Hole Patterns

Since the load-concentration factors for a mesh with a six-member hexagonal hole were lower than stress-concentration factors in an isotropic plate with a circular hole, this study was extended to examine hexagonal hole patterns that encompassed more missing members, even though occurrence of such a pattern of damage is unlikely. To proceed with the study beyond the six-member hole, only one-quarter of the full model is used because of the symmetry of the model.

Load-concentration factor as a function of  $r_h/\ell$ , where  $r_h$  is the "radius" of the hexagonal hole or radius of the circle that circumscribes the hexagon, is shown in figure 10. Data are shown for arbitrarily chosen full mesh sizes of  $8 \times 8$ ,  $16 \times 16$ ,  $24 \times 24$ ,  $32 \times 32$ , and  $40 \times 40$ . Data for the  $8 \times 8$  mesh are only determined for values of  $r_h/\ell$  equal to 1 and 2. To avoid plotting points very close to one another, data for all of the mesh sizes at values of  $r_h/\ell$  equal to 1 and 2 are not presented in figure 10. The solid line segment in the figure corresponds to results for an infinite mesh obtained by linear extrapolation of the results obtained for the two largest meshes similar to the extrapolation done in figure 8. One thing that is not apparent from figure 10 is that except for loading  $N_x$ , the relative location with respect to

the hole of the maximum loaded member may change as the hole size is increased. However, for a fixed hole size, the relative location with respect to the hole of the maximum loaded member remains unchanged as the mesh is increased.

Table III presents the load-concentration factors for all the cases, but the individual load plots for each combination of mesh number and hexagonal hole size are not presented. An example of load distribution for a hexagonal hole with radius of 4 member lengths for a  $32 \times 32$  mesh is presented in figures 11(a), 11(b), and 11(c) for the loadings,  $N_x$ ,  $N_{xy}$ , and  $N_y$ , respectively. The influence of the hole size for the loading  $N_x$  on the  $32 \times 32$  mesh is depicted in figures 12(a), 12(b), 12(c), and 11(a) for ratios of  $r_h/\ell$  of 1, 2, 3, and 4, respectively. The member loads increase as the hole extends over more rings of elements, and the effect of the hole diminishes for members farther from the hole. This is also true for the other loadings.

#### CONCLUDING REMARKS

A numerical study was conducted to examine the behavior of large space structures which have sustained damage or which have stiff equipment attached. A particular concept, the tetrahedral truss, was considered and attention was restricted to its planar faces under a series of basic loading conditions. When one member was removed near the center of the planar face of the tetrahedral truss, the maximum load in a nearby member increased by roughly 25 percent for extensional or compressive loadings and roughly 35 percent for shear loadings.

When an entire six-member unit about a particular joint at the center was removed, maximum loads increased by roughly 30 percent to 45 percent for extensional loadings, the variation being dependent upon orientation, and roughly 55 percent for shear loadings. Similarly, when a central six-member unit was replaced by a rigid insert (simulating stiff equipment), maximum member loads increased by roughly 35 percent. In general, the load-concentration effects investigated herein were found to be significantly less than the effects observed in classical stress-concentration problems for infinite plates with holes or rigid inclusions, although the effects tend to increase as a hexagonal hole extends over more rings of elements.

Langley Research Center  
National Aeronautics and Space Administration  
Hampton, VA 23665  
August 22, 1979

## REFERENCES

1. Outlook for Space. Report to the NASA Administrator by the Outlook for Space Study Group. NASA SP-386, 1976.
2. Hedgepeth, John M.: Survey of Future Requirements for Large Space Structures. NASA CR-2621, 1976.
3. Mikulas, Martin M., Jr.; Bush, Harold G.; and Card, Michael F.: Structural Stiffness, Strength and Dynamic Characteristics of Large Tetrahedral Space Truss Structures. NASA TM X-74001, 1977.
4. Bush, Harold G.; Mikulas, Martin M., Jr.; and Heard, Walter L., Jr.: Some Design Considerations for Large Space Structures. AIAA/ASME 18th Structures, Structural Dynamics and Materials Conference, Mar. 1977, pp. 186-196. (Available as AIAA Paper No. 77-395.)
5. The NASTRAN User's Manual (Level 16.0). NASA SP-222(03), 1976.
6. Giles, Gary L.: Digital Computer Programs for Generating Oblique Orthographic Projections and Contour Plots. NASA TN D-7797, 1975.
7. Isogrid Design Handbook. MDC G4295A (Contract NAS 8-28619), McDonnell Douglas Astronautics Co., Feb. 1973. (Available as NASA CR-124075.)
8. Timoshenko, S. P.; and Goodier, J. N.: Theory of Elasticity. Third Ed. McGraw-Hill Book Co., Inc., c.1970.
9. Lekhnitskii, S. G. (S. W. Tsai and T. Cheron, transl.): Anisotropic Plates. Gordon & Breach, Sci. Publ., Inc., c.1968.

TABLE I.- NONDIMENSIONAL MAXIMUM MEMBER LOADS AND LOAD-CONCENTRATION FACTORS FOR 16 x 16 MESH

Configuration	Loading $N_x$			Loading $N_{xy}$			Loading $N_y$			Loading, $N_y$ corrected		
	$\frac{P_{60}}{N_x l}$	Load-concentration factor	Classical stress-concentration factor	$\frac{P_{60}}{N_{xy} l}$	Load-concentration factor	Classical stress-concentration factor	$\frac{P_{60}}{N_y l}$	Load-concentration factor	Classical stress-concentration factor	$\frac{P_{60}}{N_y l}$	Load-concentration factor	Classical stress-concentration factor
Reference model (no missing members) . . .	0.866	1.000	1.000	-1.000	1.000	1.000	0.583	1.000	1.000	0.577	1.000	1.000
Model with horizontal member missing . . . .	1.088	1.257	-----	-1.000	1.000	-----	0.683	1.170	-----	0.680	1.178	-----
Model with diagonal member missing . . . .	0.866	1.000	-----	-1.353	1.353	-----	0.733	1.256	-----	0.725	1.256	-----
Model with six-member hexagonal hole . . .	1.130	1.304	3.000	-1.565	1.565	4.000	0.858	1.470	3.000	0.853	1.478	3.000
Model with hexagonal rigid insert . . . .	1.157	1.336	1.500	-1.279	1.279	1.500	0.796	1.365	1.500	0.787	1.364	1.500

TABLE II.- NONDIMENSIONAL MAXIMUM MEMBER LOADS FOR STRUCTURE  
CONTAINING SIX-MEMBER HEXAGONAL HOLE

Mesh size	Loading $N_x$	Loading $N_{xy}$	Loading $N_y$	Loading, $N_y$ corrected
	$\frac{P_{00}}{N_x \ell}$	$\frac{P_{-600}}{N_{xy} \ell}$	$\frac{P_{600}}{N_y \ell}$	$\frac{P_{600}}{N_y \ell}$
4 × 4	1.3712	-2.0000	1.1547	1.0104
8 × 8	1.1863	-1.6641	.9095	.8971
16 × 16	1.1297	-1.5649	.8583	.8535
24 × 24	1.1193	-1.5453	.8480	.8442
28 × 28	1.1170	-1.5411	.8456	.8422
32 × 32	1.1156	-1.5383	.8439	.8408
40 × 40	1.1139	-1.5350	.8418	.8393

TABLE III.- LOAD-CONCENTRATION FACTORS FOR STRUCTURE  
CONTAINING HEXAGONAL HOLES

Mesh size	Hole size, $r_h/l$	Load-concentration factors for -			
		Loading $N_x$	Loading $N_{xy}$	Loading $N_y$	Loading, $N_y$ corrected
8 × 8	1	1.370	1.664	1.529	1.554
	2	2.325	2.631	2.997	2.989
16 × 16	1	1.304	1.565	1.470	1.478
	2	1.752	1.975	2.282	2.286
	3	2.281	2.777	3.330	3.342
	4	3.078	4.043	4.931	4.955
24 × 24	1	1.292	1.545	1.457	1.462
	2	1.658	1.846	2.161	2.162
	3	1.985	2.358	2.881	2.886
	4	2.370	3.019	3.711	3.720
32 × 32	1	1.288	1.538	1.453	1.456
	2	1.626	1.800	2.118	2.119
	3	1.890	2.217	2.733	2.736
	4	2.160	2.694	3.352	3.357
40 × 40	1	1.286	1.535	1.451	1.454
	2	1.612	1.779	2.098	2.099
	3	1.848	2.152	2.665	2.668
	4	2.069	2.550	3.194	3.198

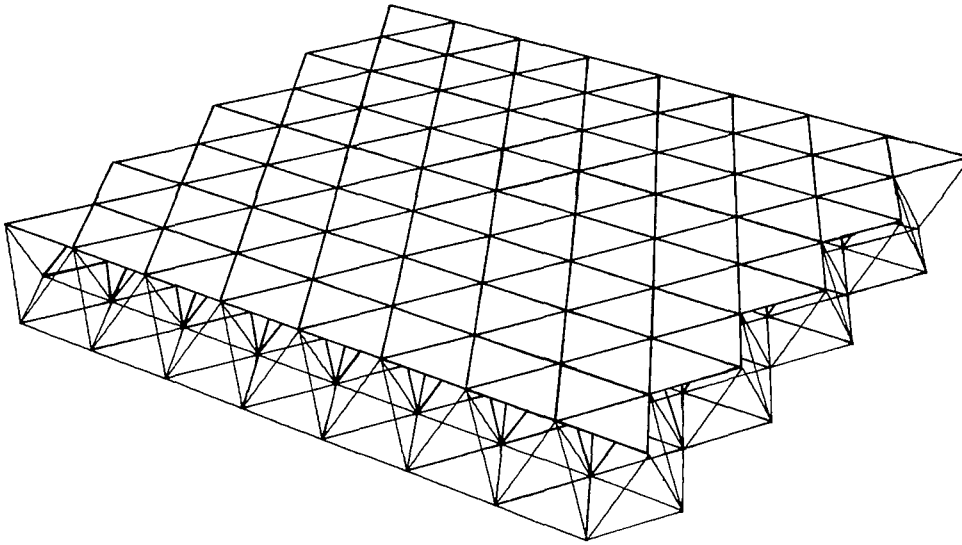


Figure 1.- Model of a portion of a tetrahedral truss.

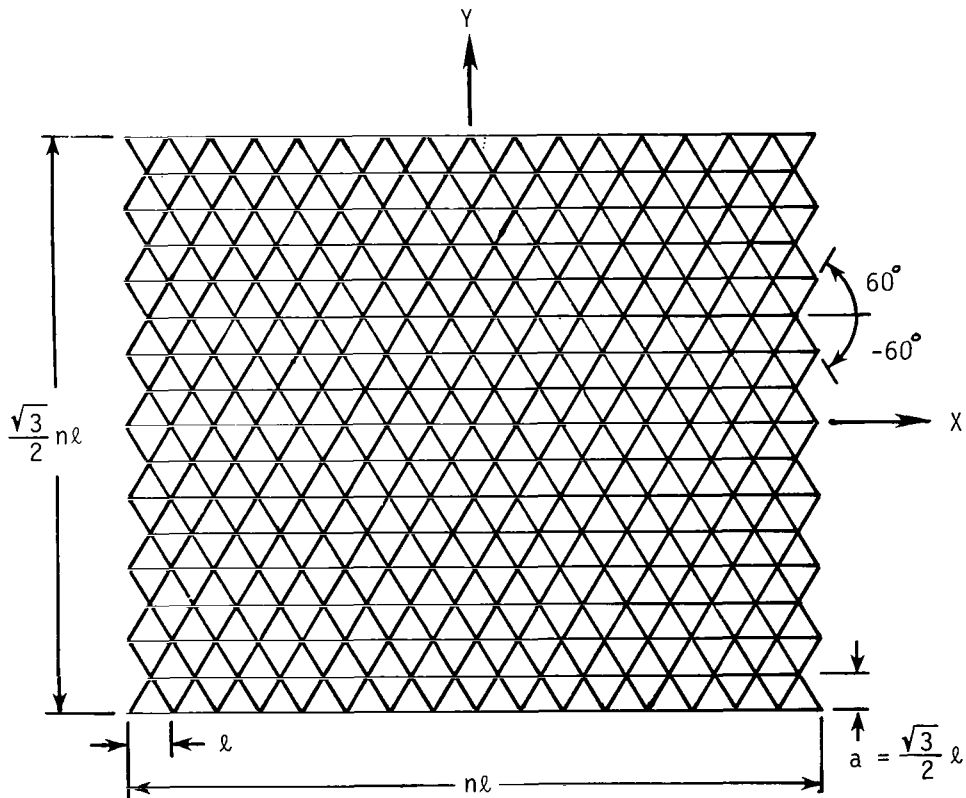
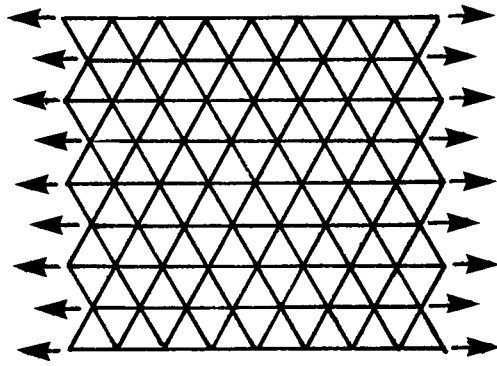
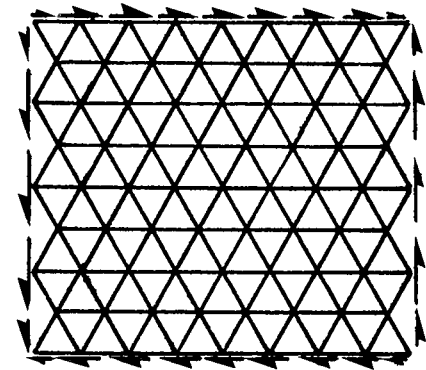
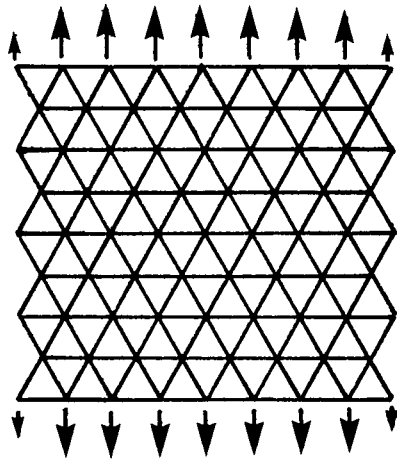
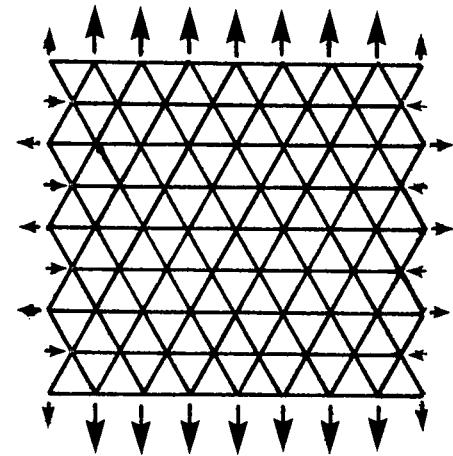


Figure 2.- Coordinate system and layout of  $n \times n$  mesh for planar face of a tetrahedral truss.

(a)  $N_x$ .(b)  $N_{xy}$ .(c)  $N_y$ .(d)  $N_y$  corrected.Figure 3.- Basic loading conditions (shown for  $8 \times 8$  mesh).

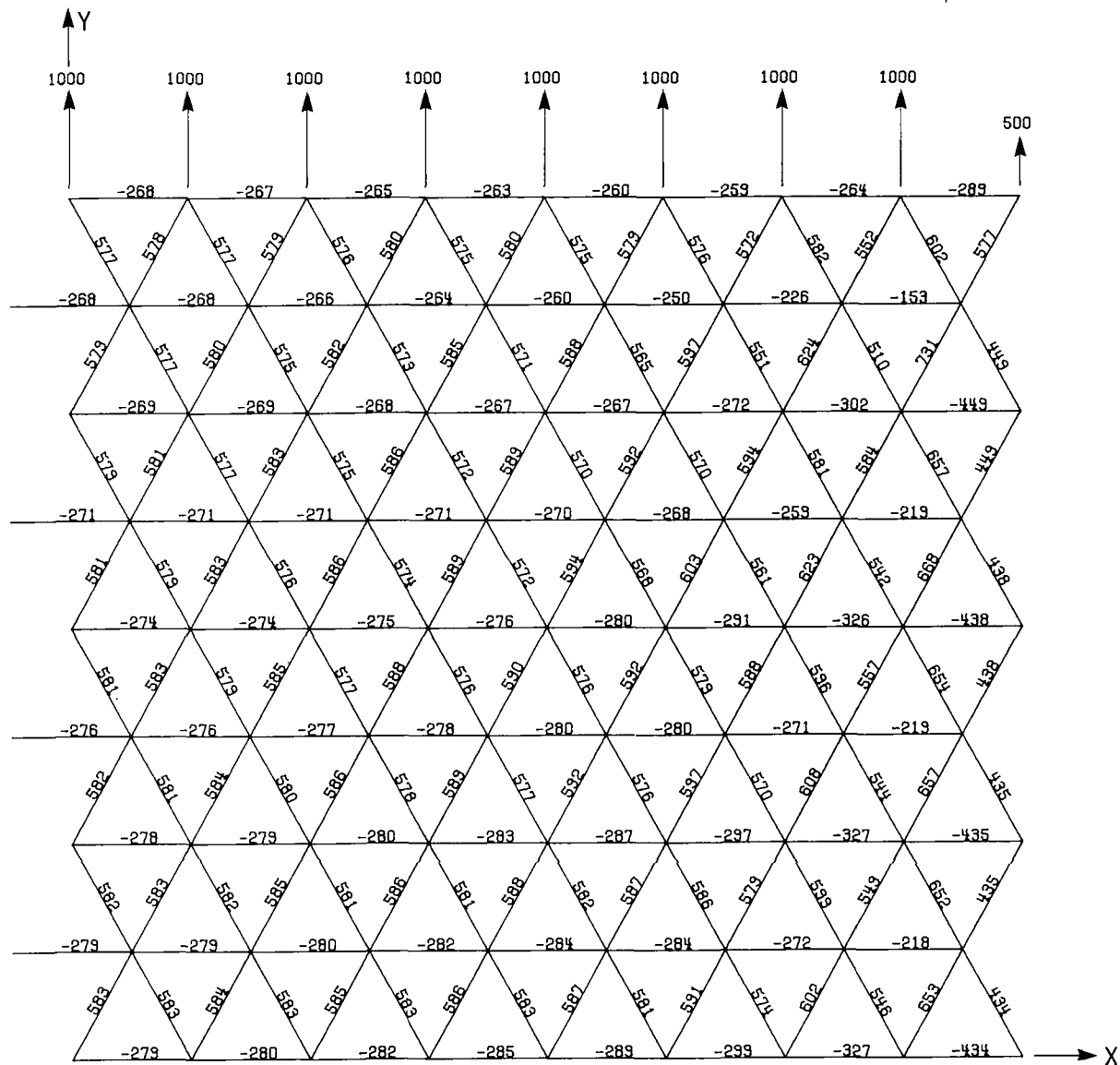


Figure 4.- Nondimensional member loads in 16 x 16 mesh structure due to loading  $N_y$ . Only one quadrant shown.

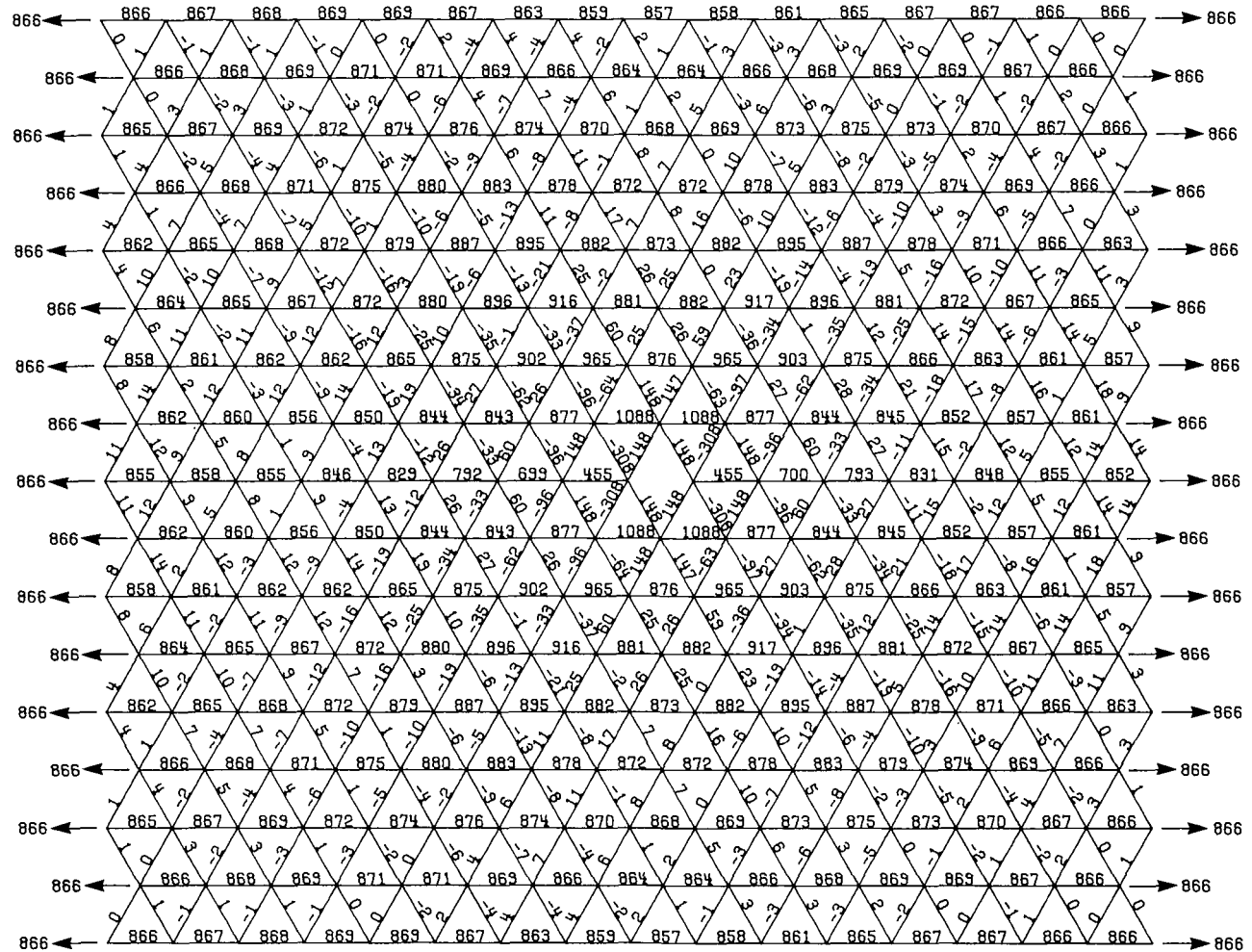
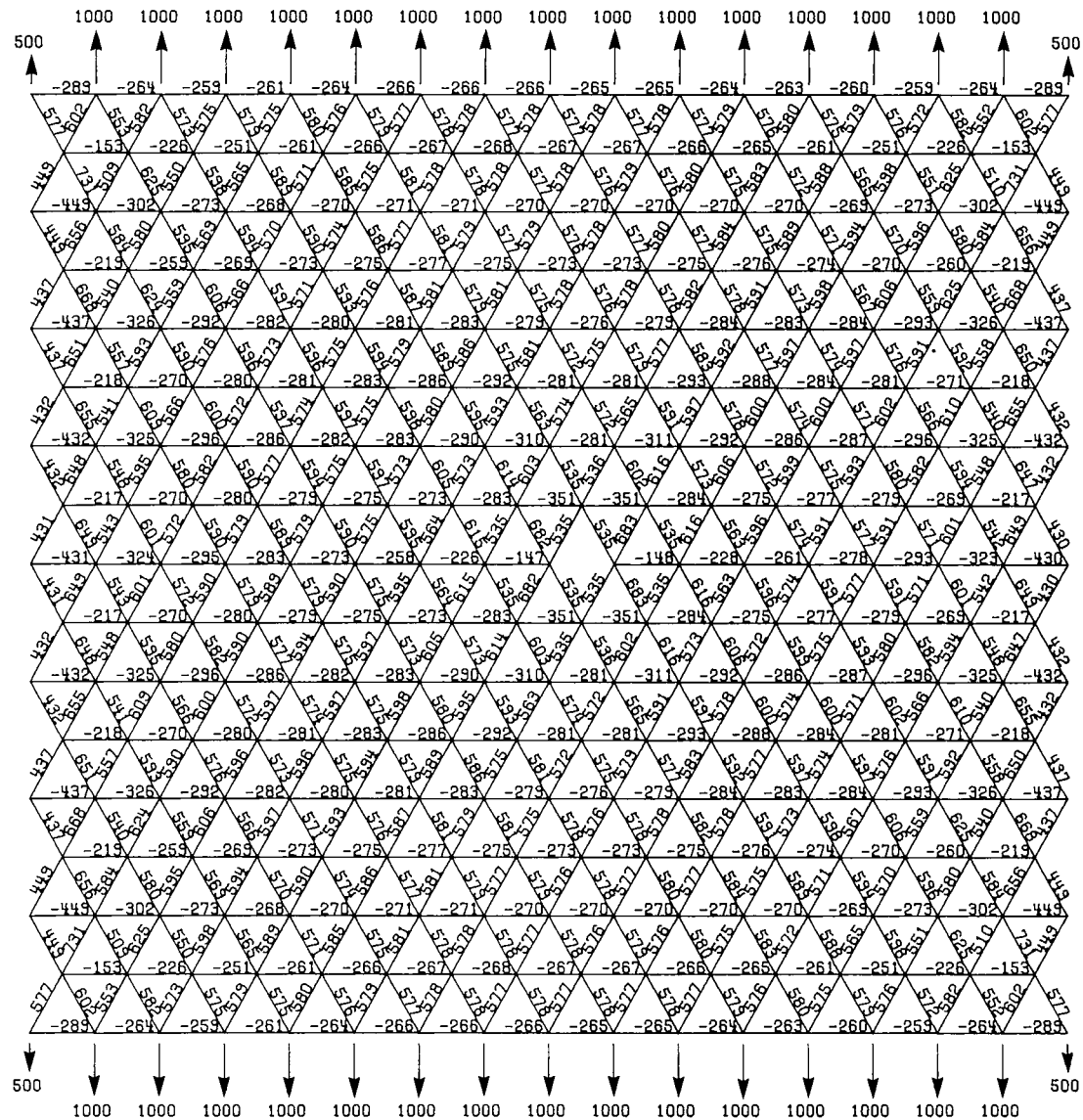
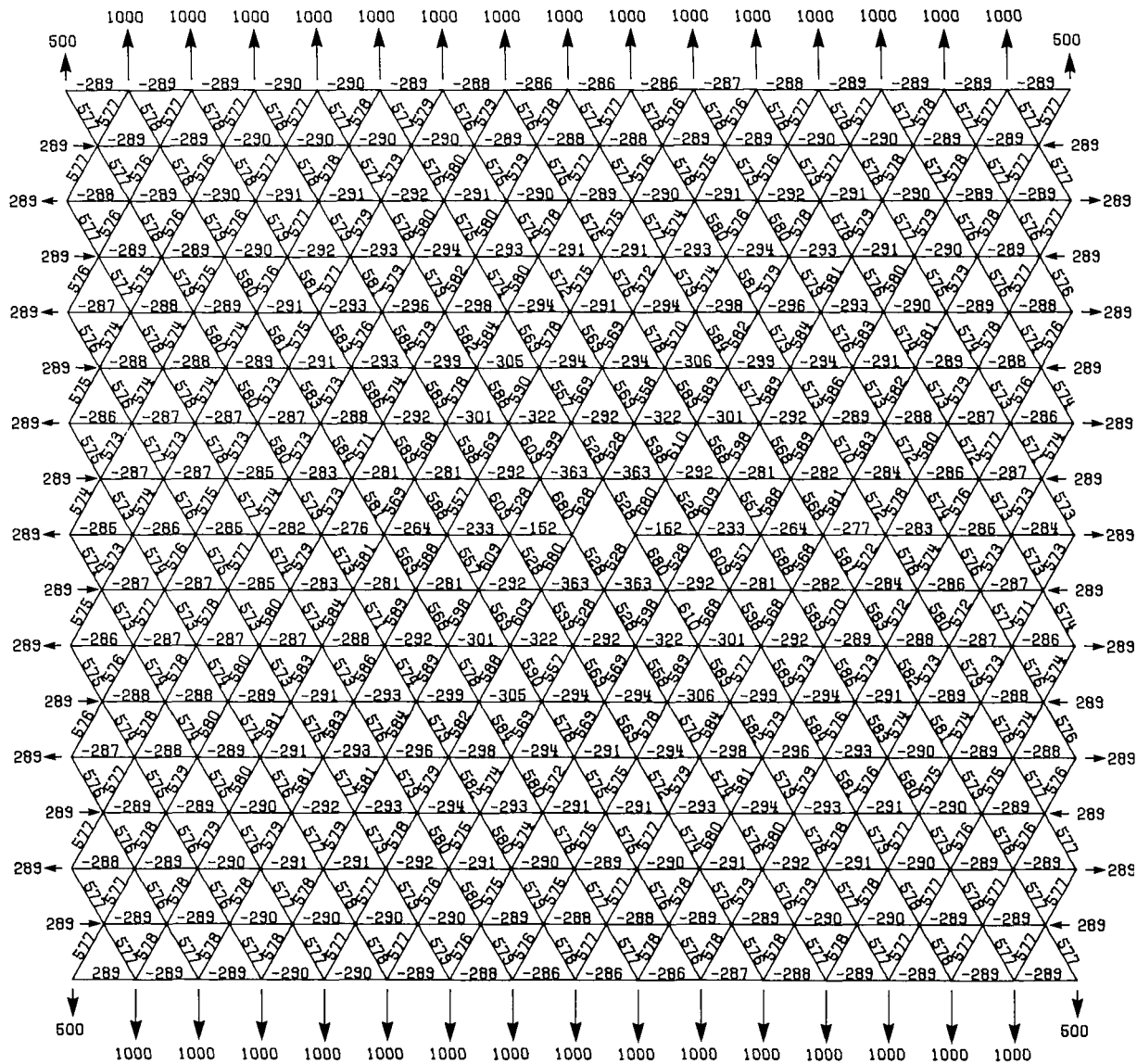
(a) Loading  $N_x$ .

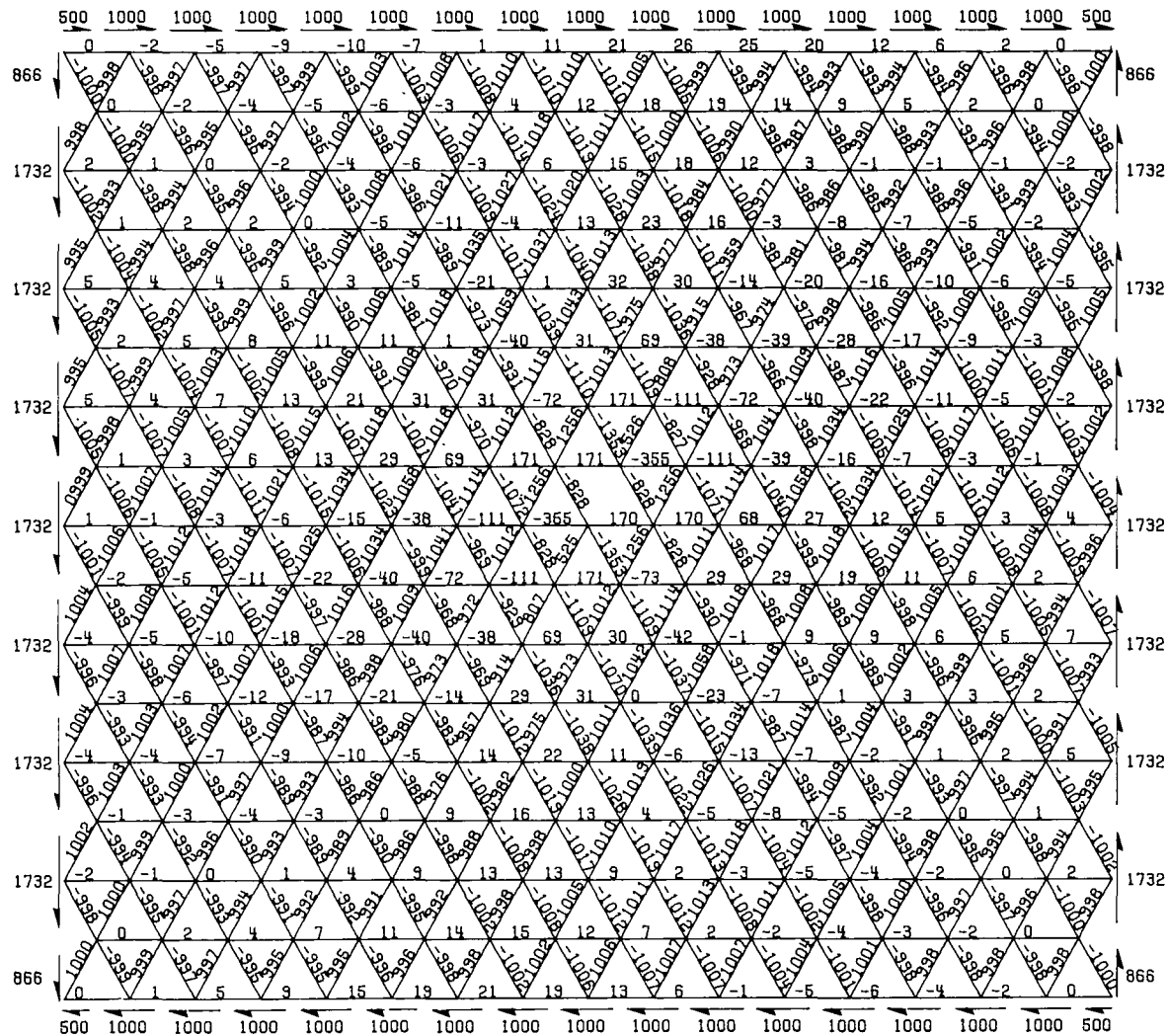
Figure 5.- Nondimensional member loads in a 16 x 16 mesh structure with horizontal member missing near center.





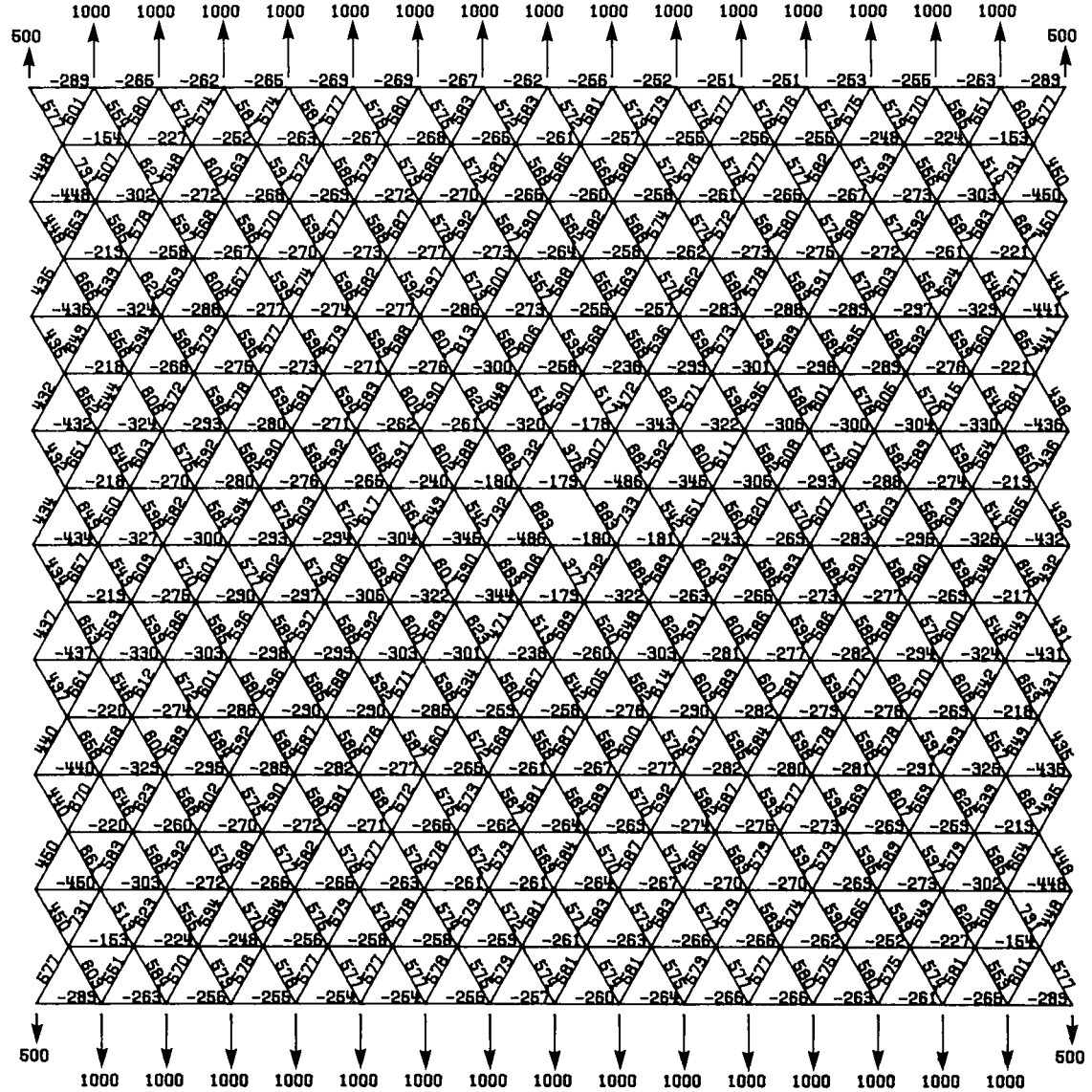
(c) Loading,  $N_y$  corrected.

Figure 5.- Concluded.



(a) Loading  $N_{xy}$ .

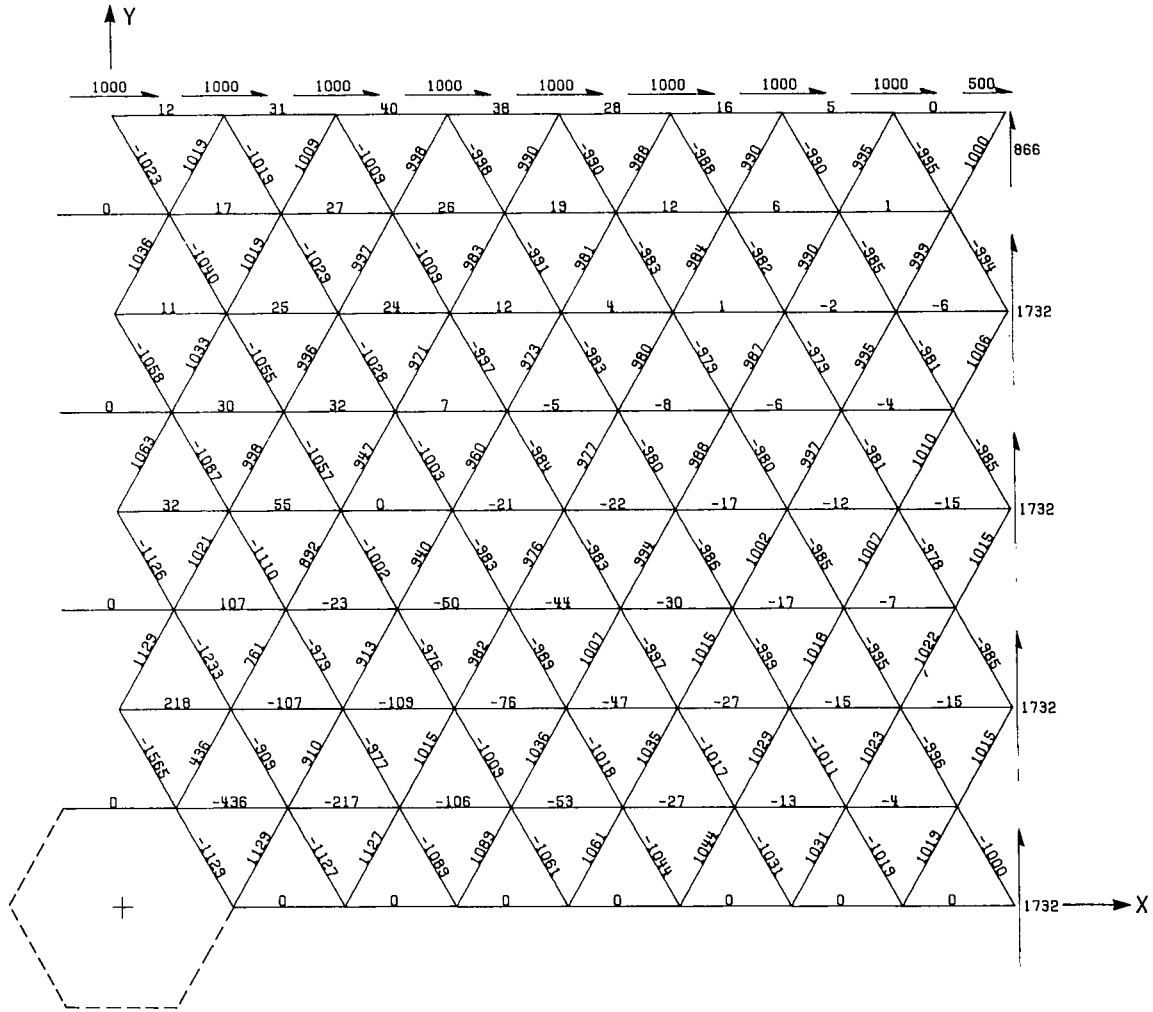
Figure 6.- Nondimensional member loads in  $16 \times 16$  mesh structure with diagonal member missing near center.



(b) Loading  $N_y$ .

Figure 6.- Concluded.





(b) Loading  $N_{xy}$ .

Figure 7.- Continued.



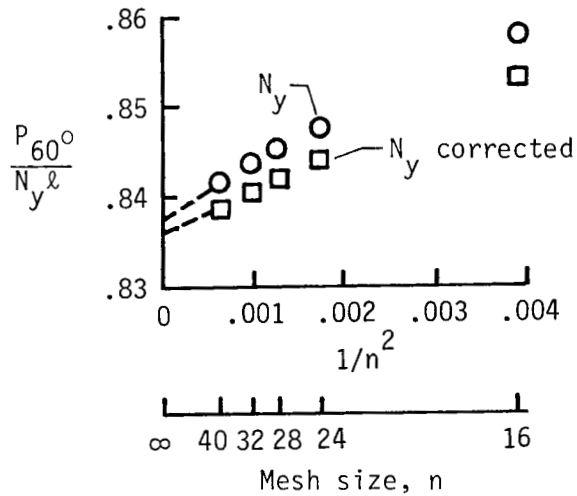
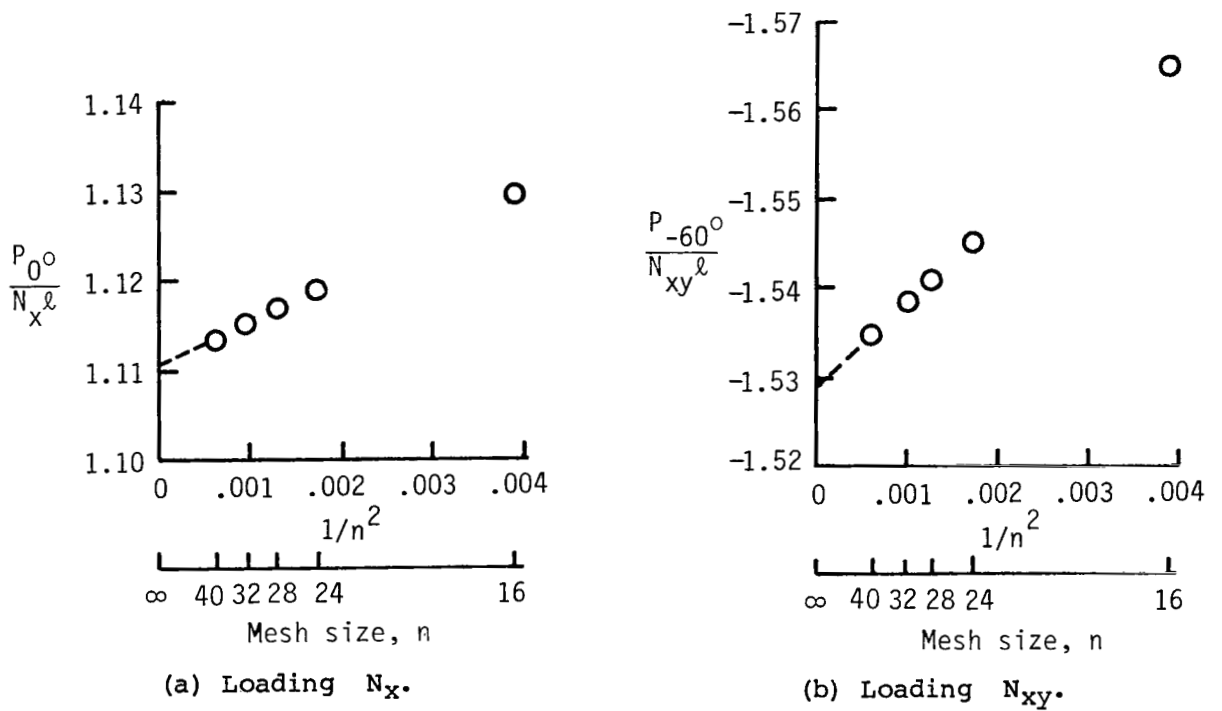
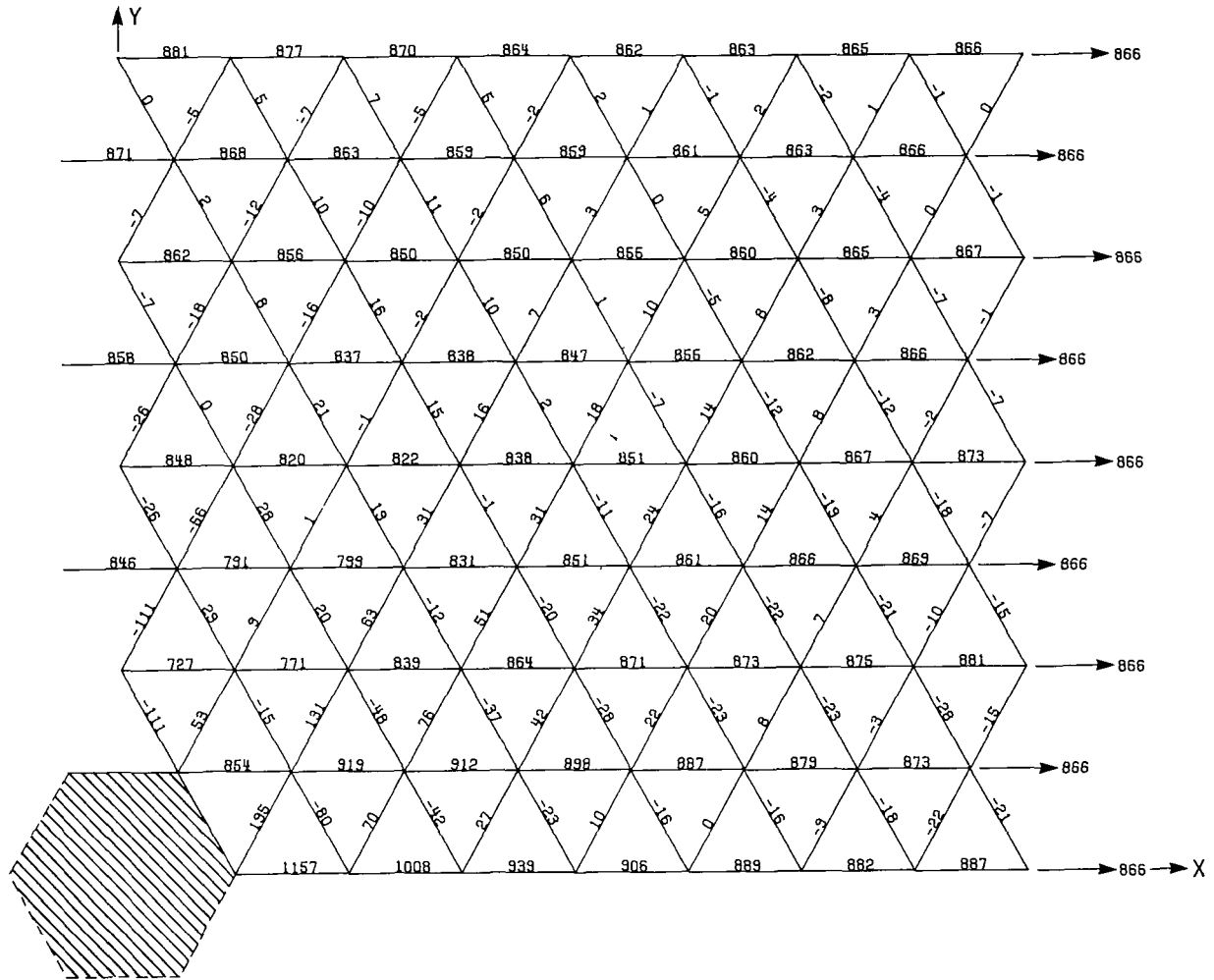
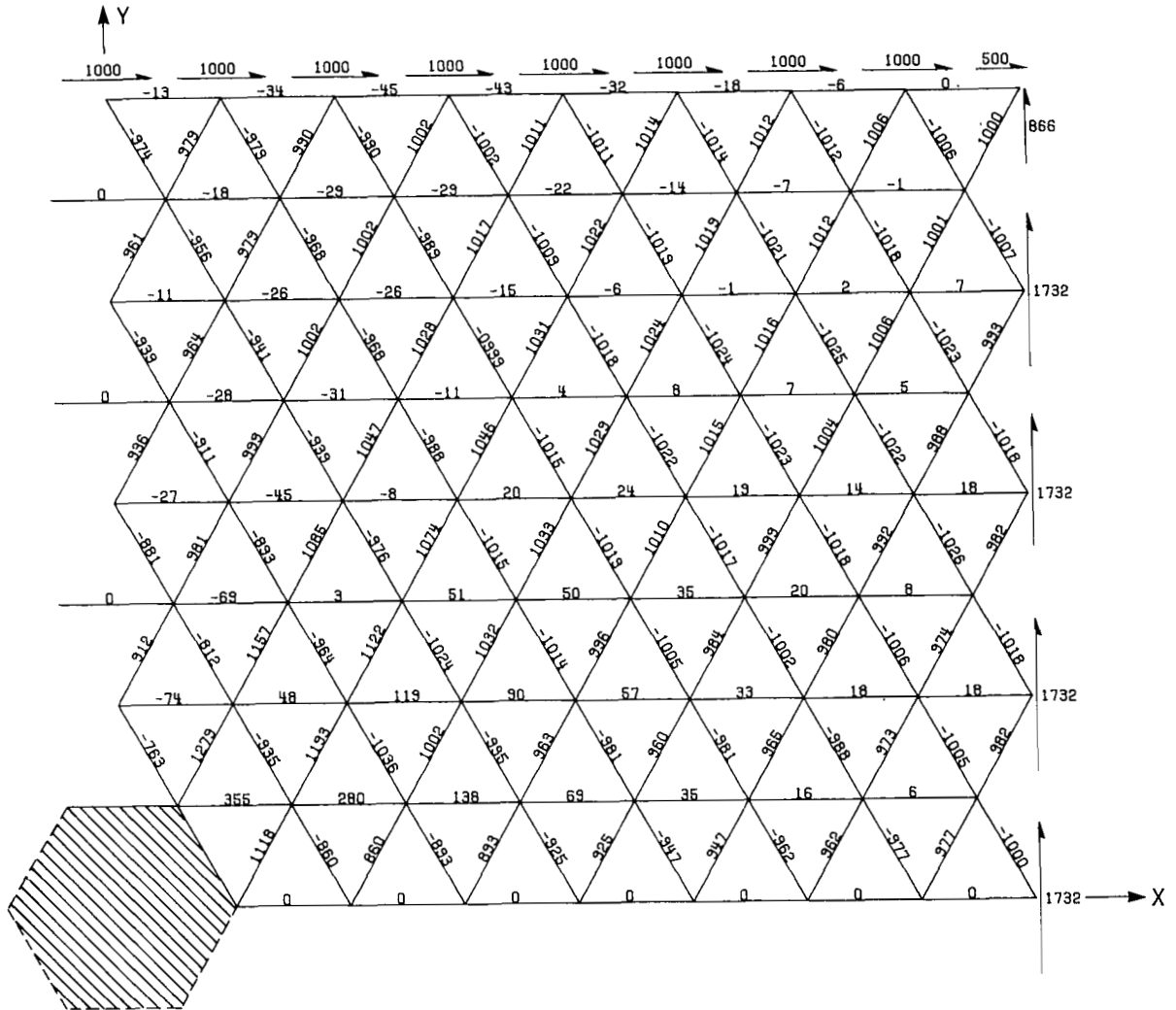


Figure 8.- Maximum nondimensional member loads for structure with six-member hexagonal hole as function of mesh size.  $r_H/l = 1.0$ .



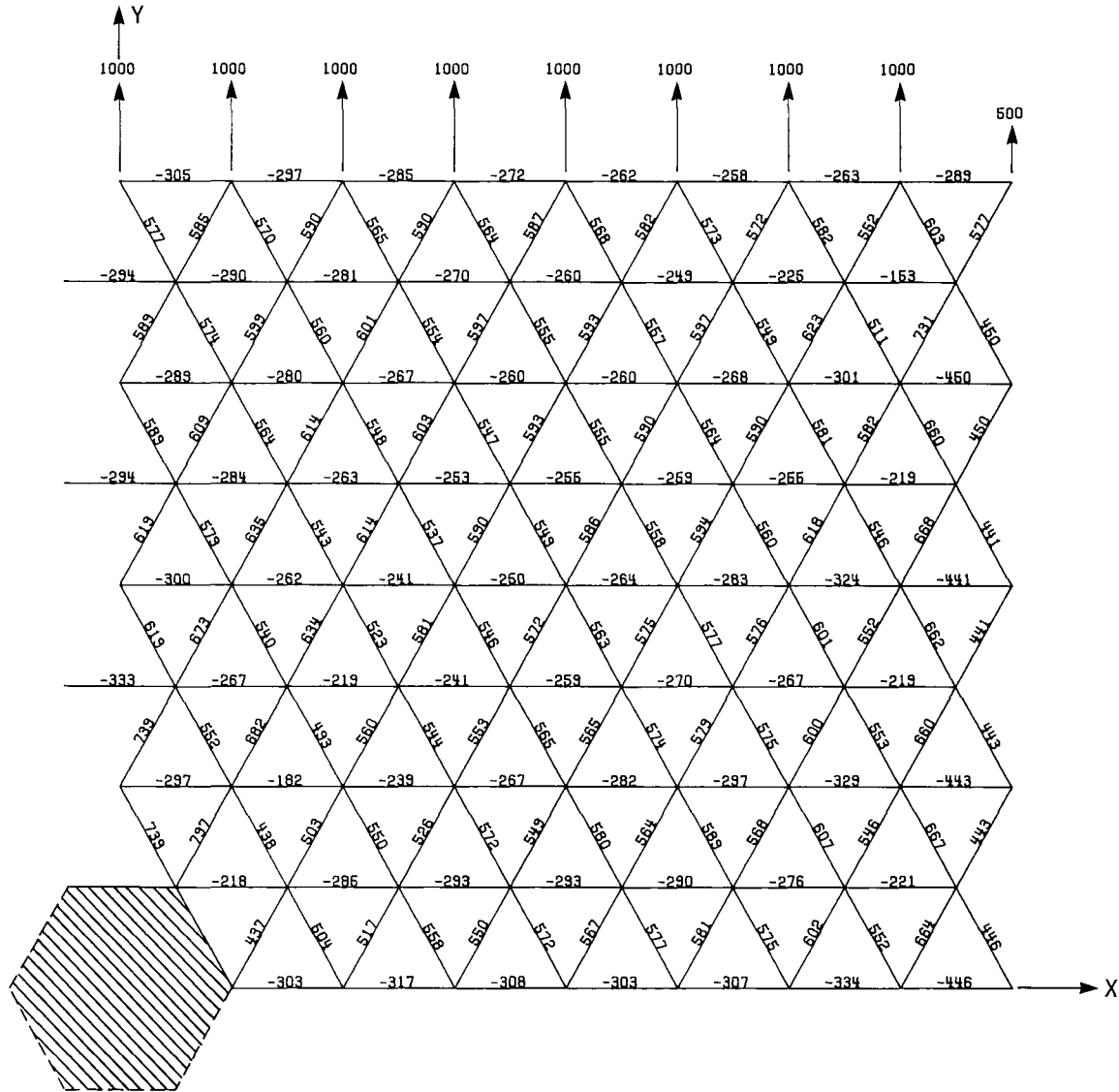
(a) Loading  $N_x$ .

Figure 9.- Nondimensional member loads in  $16 \times 16$  mesh structure with rigid hexagonal insert at center. Only one quadrant shown.



(b) Loading  $N_{xy}$ .

Figure 9.- Continued.



(c) Loading  $N_y$ .

Figure 9.- Concluded.

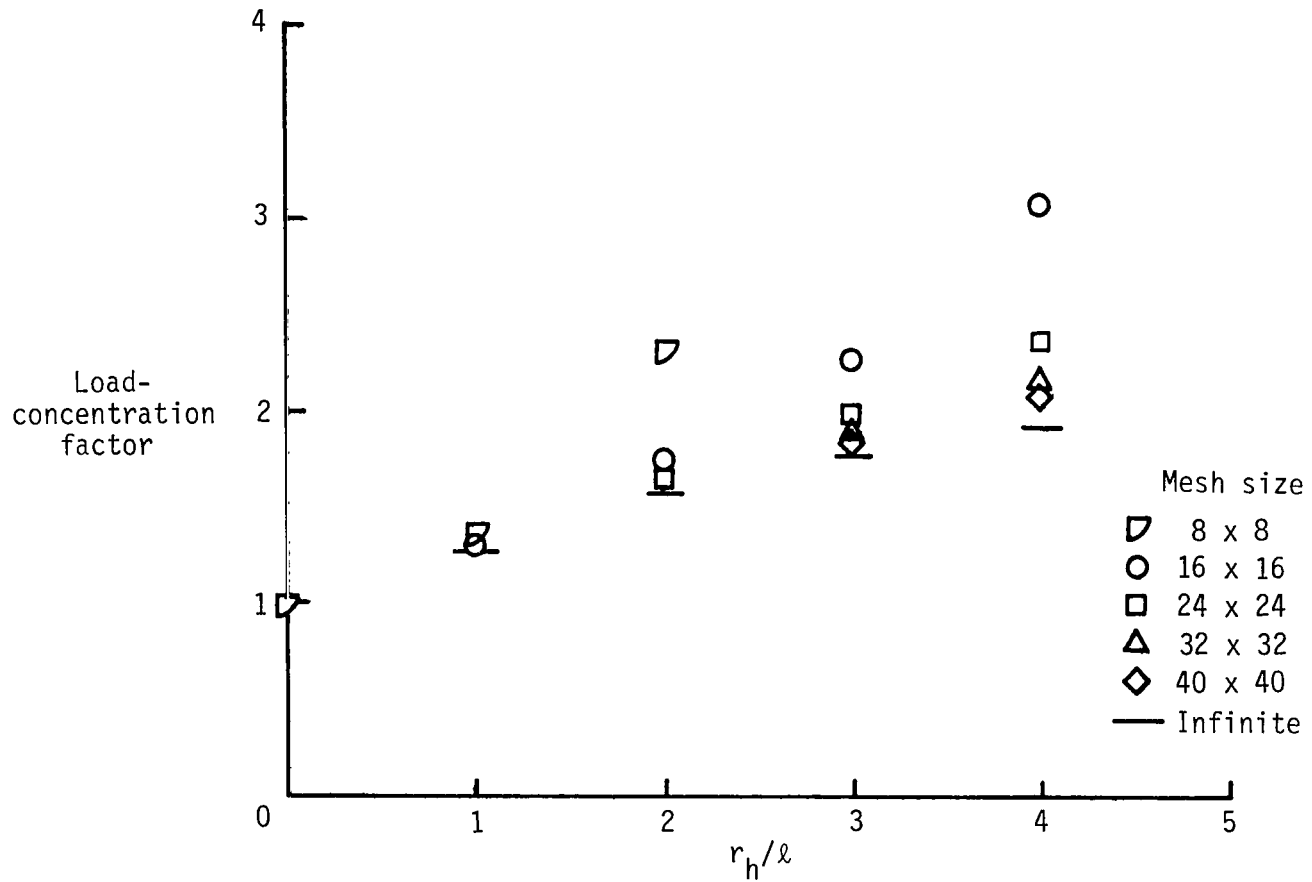
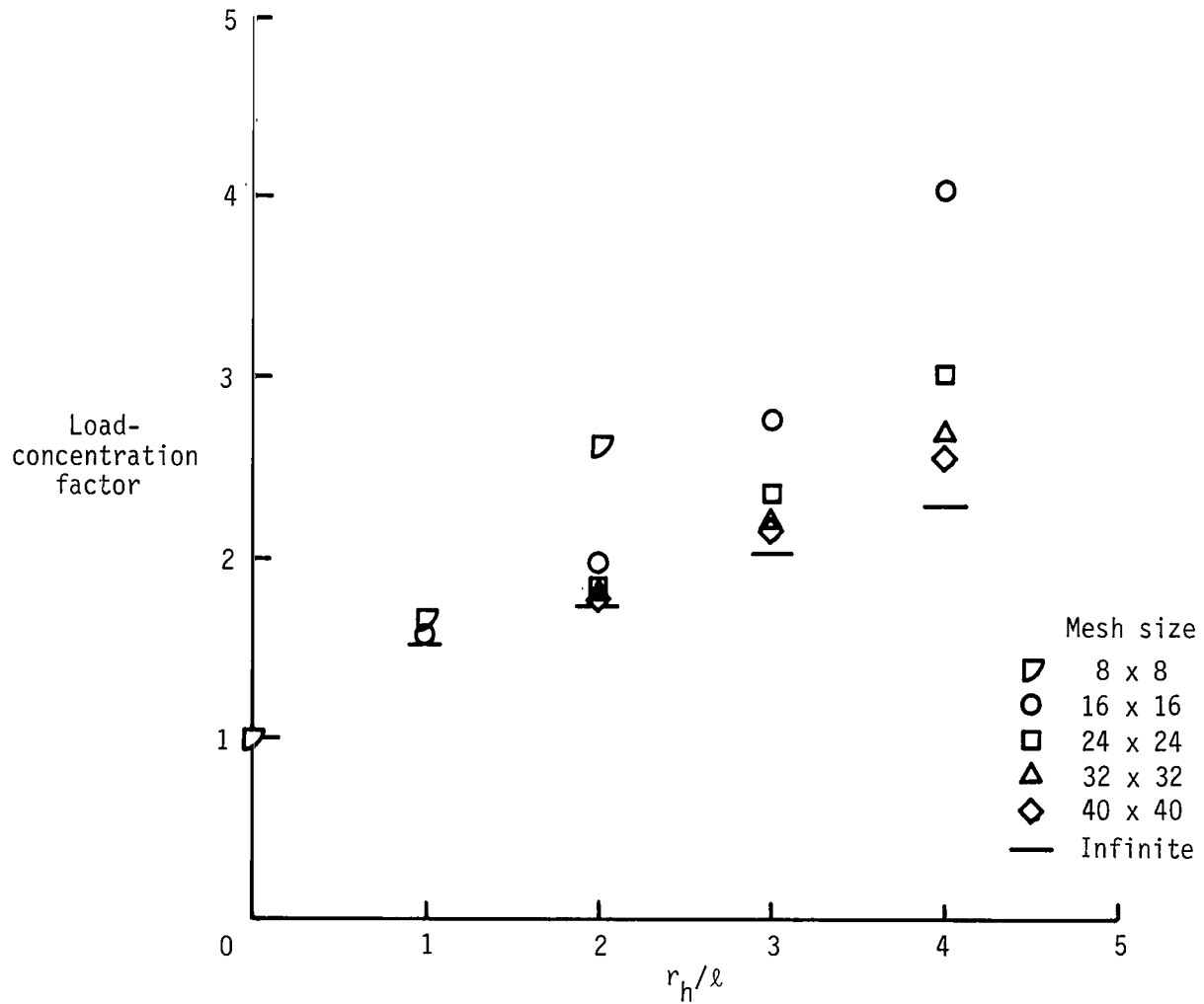
(a) Loading  $N_x$ .

Figure 10.- Load-concentration factor as function of hexagonal hole size.



(b) Loading  $N_{xy}$ .

Figure 10.- Continued.

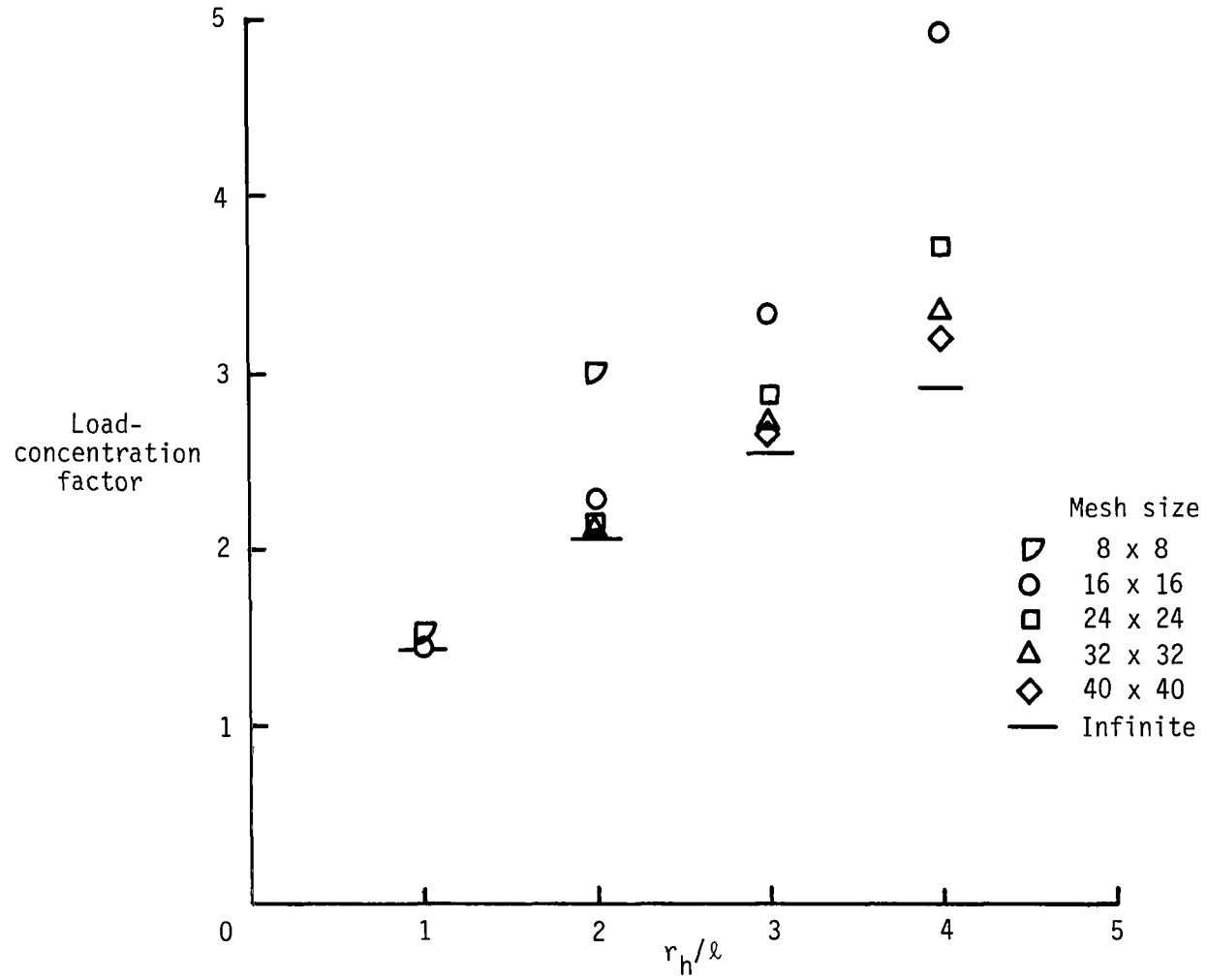
(c) Loading  $N_y$ .

Figure 10.- Concluded.

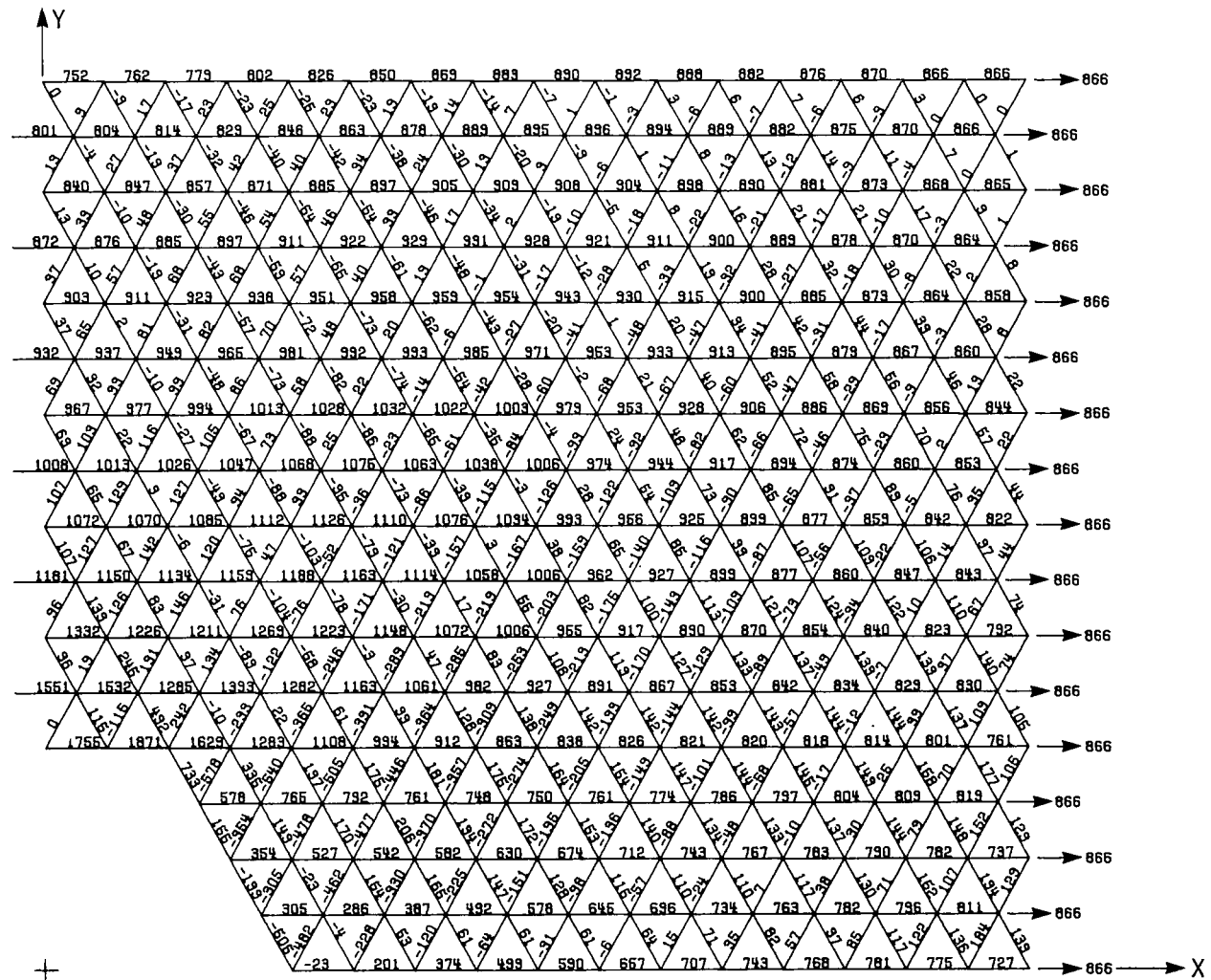
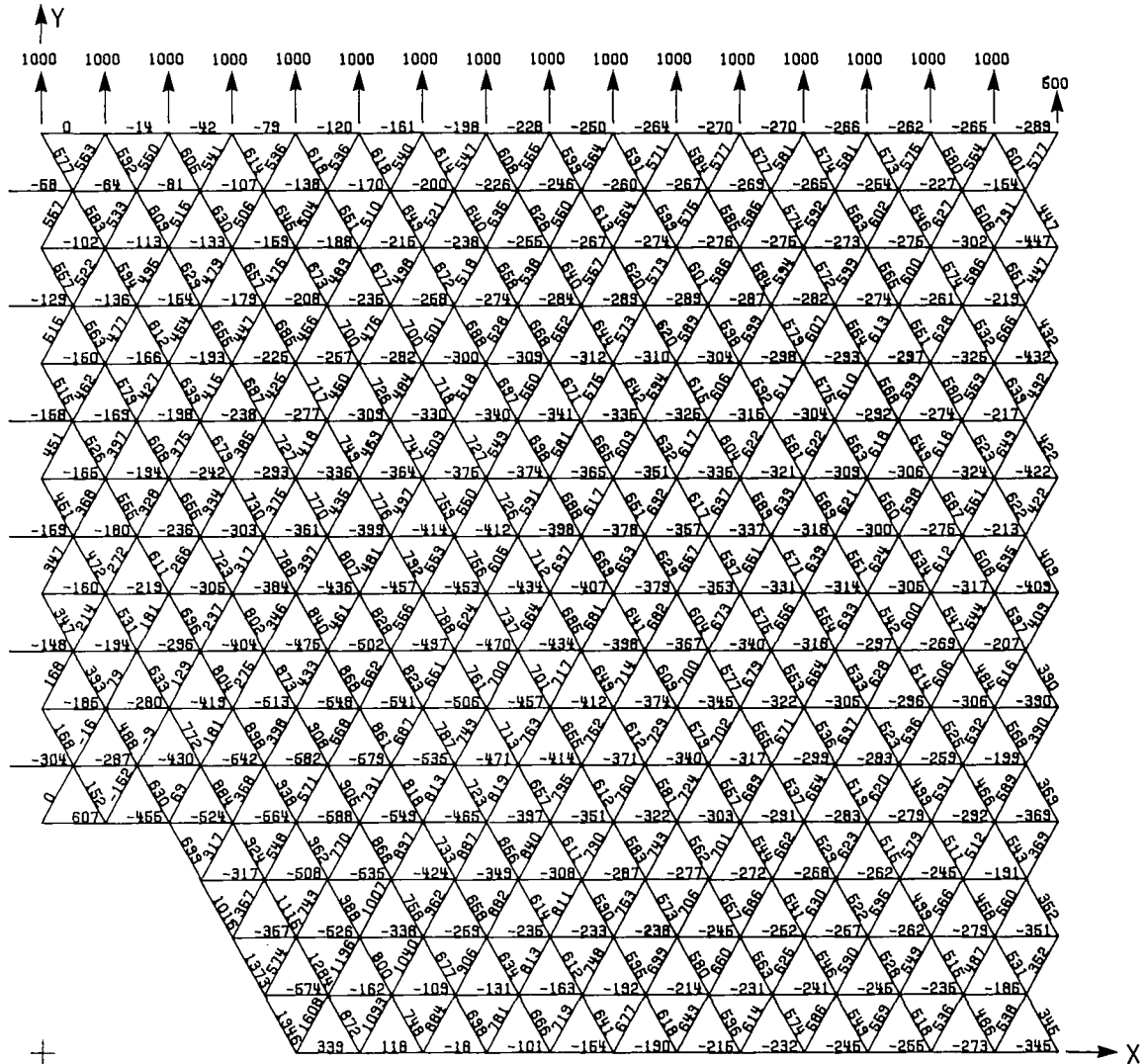


Figure 11.- Nondimensional member loads in  $32 \times 32$  mesh structure with hexagonal hole extending over four rings of elements. Only one quadrant shown.

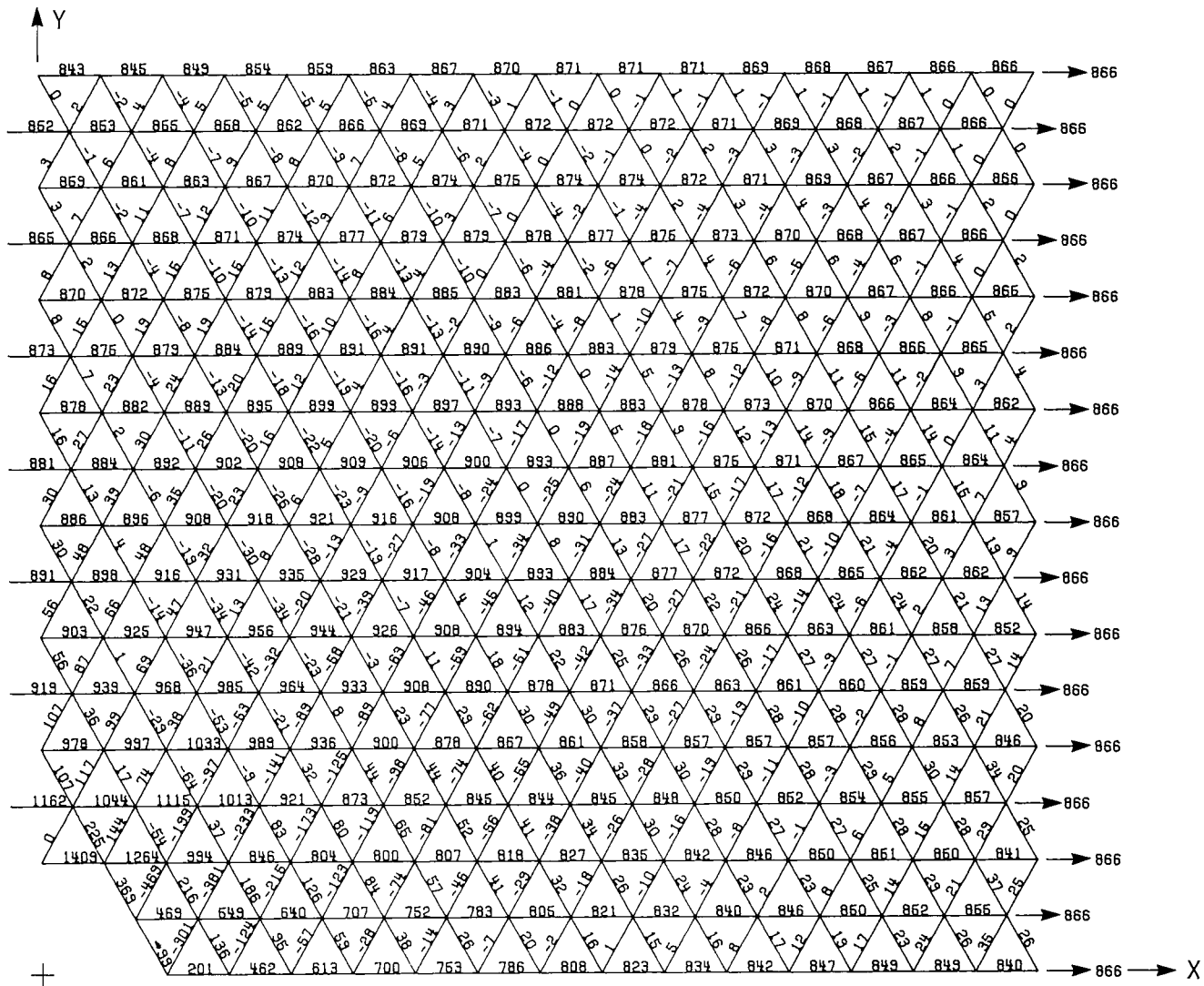




(c) Loading  $N_y$ .

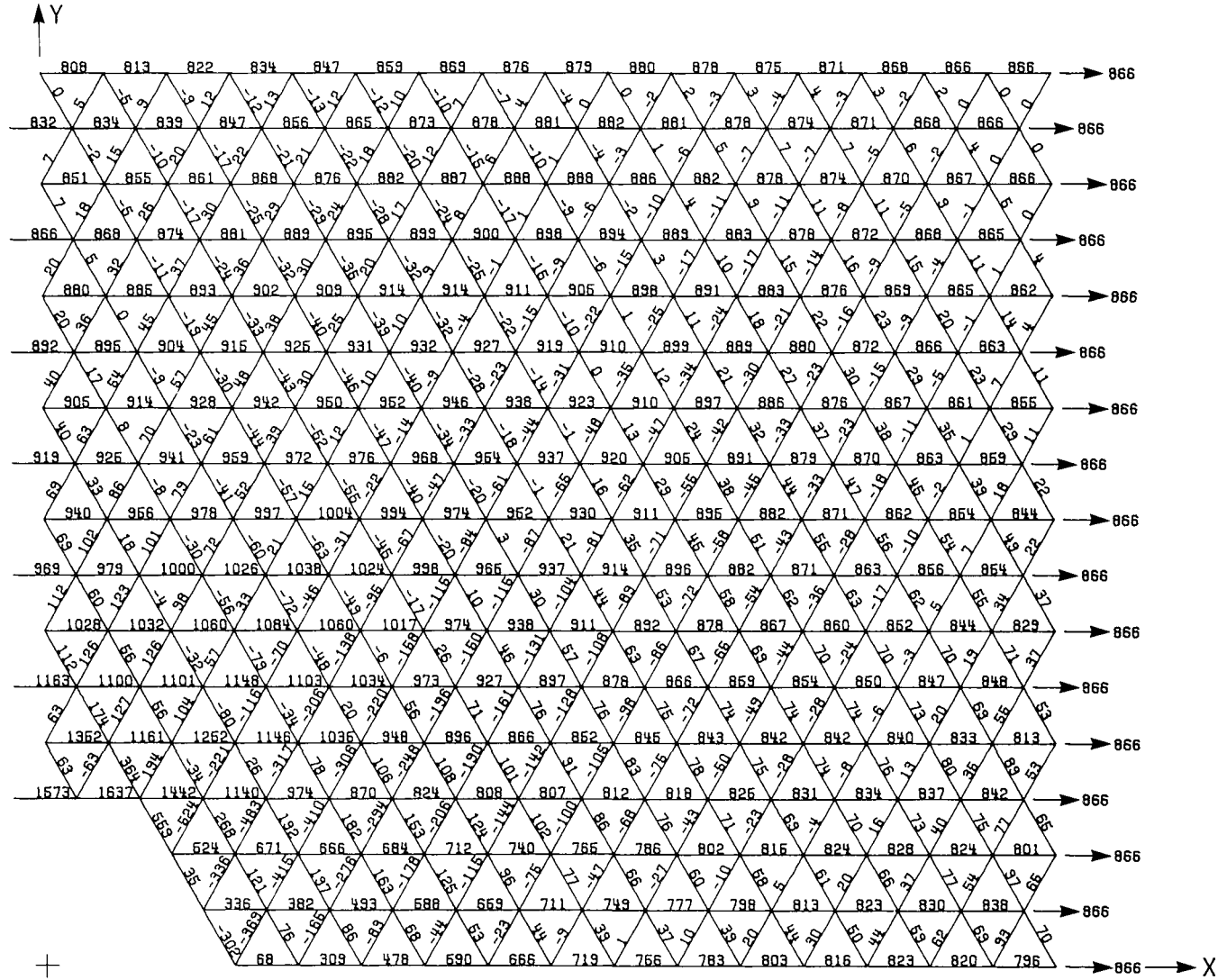
Figure 11.- Concluded.





(b) Hexagonal hole extending over two rings of elements.

Figure 12.- Continued.



(c) Hexagonal hole extending over three rings of elements.

Figure 12.- Concluded.

1. Report No. NASA TP-1522		2. Government Accession No.		3. Recipient's Catalog No.	
4. Title and Subtitle LOAD CONCENTRATION DUE TO MISSING MEMBERS IN PLANAR FACES OF A LARGE SPACE TRUSS				5. Report Date October 1979	
				6. Performing Organization Code	
7. Author(s) Joseph E. Walz				8. Performing Organization Report No. L-12872	
				10. Work Unit No. 506-17-13-20	
9. Performing Organization Name and Address NASA Langley Research Center Hampton, VA 23665				11. Contract or Grant No.	
				13. Type of Report and Period Covered Technical Paper	
12. Sponsoring Agency Name and Address National Aeronautics and Space Administration Washington, DC 20546				14. Sponsoring Agency Code	
15. Supplementary Notes					
16. Abstract  A large space structure with members missing was investigated using a finite-element analysis. The particular structural configuration was the tetrahedral truss, with attention restricted to one of its planar faces. Initially the finite-element model of a complete face was verified by comparing it with known results for some basic loadings. Then an analysis was made of the structure with members near the center removed. Some calculations were made on the influence of the mesh size of a structure containing a hexagonal hole, and an analysis was also made of a structure with a rigid hexagonal insert. In general, load-concentration effects in these trusses were significantly lower than classical stress-concentration effects in an infinitely wide isotropic plate with a circular rigid inclusion, although larger effects were obtained when a hole extended over several rings of elements.					
17. Key Words (Suggested by Author(s)) Load concentration Large space structures Stress concentration Tetrahedral truss Missing truss members			18. Distribution Statement Unclassified - Unlimited  Subject Category 39		
19. Security Classif. (of this report) Unclassified	20. Security Classif. (of this page) Unclassified	21. No. of Pages 36	22. Price* \$4.50		

\* For sale by the National Technical Information Service, Springfield, Virginia 22161

NASA-Langley, 1979

National Aeronautics and  
Space Administration

THIRD-CLASS BULK RATE

Postage and Fees Paid  
National Aeronautics and  
Space Administration  
NASA-451



Washington, D.C.  
20546

Official Business

Penalty for Private Use, \$300

4 1 1U,D, 092479 S00903DS  
DEPT OF THE AIR FORCE  
AF WEAPONS LABORATORY  
ATTN: TECHNICAL LIBRARY (SUL)  
KIRTLAND AFB NM 87117

**NAS**

**S**

POSTMASTER: If Undeliverable (Section 158  
Postal Manual) Do Not Return